

## ON THE STARK BROADENING OF B IV SPECTRAL LINES

MILAN S. DIMITRIJEVIĆ<sup>1,2</sup>, MAGDALENA CHRISTOVA<sup>3</sup>, ZORAN SIMIĆ<sup>1</sup>,  
ANDJELKA KOVACHEVIĆ<sup>4</sup>, SYLVIE SAHAL-BRÉCHOT<sup>2</sup>

<sup>1</sup>*Astronomical Observatory, Volgina 7, 11060 Belgrade 38, Serbia*

<sup>2</sup>*Observatoire de Paris, 92195 Meudon Cedex, France*

<sup>3</sup>*Department of Applied Physics, Technical University-Sofia, 1000 Sofia, Bulgaria*

<sup>4</sup>*Department of Astronomy, Faculty of Mathematics, Studentski Trg 16,  
11000 Belgrade, Serbia.*

E-mail: mdimitrijevic@aob.rs, mchristo@tu-sofia.bg, zsimic@aob.rs,  
andjelka@matf.bg.ac.rs, sylvie.sahal-brechot@obspm.fr

**Abstract.** The preliminary results for Stark broadening parameters of B IV lines from 8 spectral series have been calculated using Sahal-Bréchot theory based on the semi-classical perturbation formalism.

### 1. INTRODUCTION

A major interest consists in the understanding of the evolution of the Universe, of the birth, growing, evolution and death of stars, which eject their material into the interstellar medium at the end of their life. The light trace elements lithium, beryllium, and boron (LiBeB) are at the centre of astrophysical puzzles involving sites as diverse as the primordial fireball, interstellar (IS) or even intergalactic space, and stellar surfaces and interiors (Venn et al., 2002). The origins of the light element trio are connected, by varying degrees, to the big bang nucleosynthesis, cosmic-ray spallation, and stellar evolution. Abundance determinations of Li, Be, and B in a variety of stars provide data on the above astrophysical processes that can both produce and destroy these rare elements. The light elements are sensitive probes of stellar models due to the fact that the stable isotopes of all three consist of nuclei with small binding energies that are destroyed easily by (p, a) reactions at modest temperatures (Cunha and Smith, 1999). The origin and evolution of boron are of special interest because it is hardly produced by the standard big bang nucleosynthesis (BBN), and cannot be produced by nuclear fusion in stellar interiors (Tan, Shi and Zhao, 2010). The light isotopes  $^{10}\text{B}$  and  $^{11}\text{B}$  are believed to be primarily formed via spallation of carbon and oxygen nuclei (Proffitt et al.,

1999). Traditional models for this process (Meneguzzi, Audouze and Reeves, 1971), where cosmic ray protons and alpha-particles collide with pre-existing CNO nuclei in the interstellar medium, predicted that beryllium and boron would scale quadratically with the overall metal abundance and that the ratio  $^{11}\text{B}/^{10}\text{B} \approx 2.5$ . However, boron and beryllium abundances actually scale linearly with the total metal abundance, and it has long been known that the meteoritic ratio of  $^{11}\text{B}/^{10}\text{B} \approx 4$  (Proffitt et al., 1999, Meneguzzi, Audouze and Reeves, 1971, Duncan, Lambert and Lemke, 1992, Duncan et al., 1997, Shima, 1963). These papers are concerned primarily with boron's role in testing models of stellar interiors and evolution. This role arises because boron nuclei are destroyed by warm protons, and thus even quite shallow mixing of the atmosphere with the interior reduces the surface abundance by bringing boron-depleted material to the surface. Lithium and beryllium are similarly affected. Thus, a determination that the surface abundance of a light element is less than the star's initial abundance is an observational constraint for testing models of stellar interiors (Venn et al., 2002).

Boron alone is observable in hot stars. A principal goal of most of studies of hot stars was to establish the present-day boron abundance in order to improve the understanding of the Galactic chemical evolution of boron (Venn et al., 2002). In Tan, Shi and Zhao (2010) has been reported that, the abundances of the nine stars which are not depleted in Be or B show that, no matter what the strength of collisions with neutral hydrogen may be, both Be and B increase with O quasilinearly in the logarithmic plane, which confirms the conclusions that Be and B are mainly produced by the primary process in the early Galaxy. Boron in hot stars, like lithium in cool stars, is shown to be a tracer of some of the various processes affecting a star's surface composition that are not included in the standard models of stellar evolution. If the initial boron abundances of local hot stars are similar from star to star and association to association, then the large spread in boron abundances shows that boron abundances are a clue to unravelling the nonstandard processes that affect young hot stars.

The cosmic abundances of  $^{11}\text{B}$  is of major importance for the model of Galactic chemical evolution (GCE) (Ritchey et al., 2011), where the authors conclude that a major portion of the cosmic abundances of  $^{11}\text{B}$  can be attributed to neutrino nucleosynthesis. Thus, it is necessary to accurately describe the stellar evolution, and the formation of elements, which are closely connected. To make progress in these developments chemical abundances are crucial parameters to be determined. This needs an accurate interpretation of the detailed line spectra of the stellar objects.

## 2. STARK BROADENING OF BORON LINES

Pressure broadening of spectral lines arises when an atom, ion, or molecule which emits or absorbs light in a gas or plasma, is perturbed by its interactions with the other particles of the medium. Interpretation of this phenomenon is currently used for modelling of the medium and for spectroscopic diagnostics, since the broadening of the lines depends on the temperature and density of the

medium. The physical conditions in the Universe are very various, and collisional broadening with charged particles (Stark broadening) appears to be important in many domains. For example, at temperatures around  $10^4$  K and densities  $10^{13}$  -  $10^{15}$  cm $^{-3}$ , Stark broadening is efficient for modelling and analysing spectra of moderately hot (A), hot (B) and very hot (O) types of stars Sahal-Bréchot, 2010). In white dwarfs, especially, Stark broadening is the dominant collisional line broadening process. The theory of Stark broadening is well applied, especially for accurate spectroscopic diagnostics and modelling. This requires the knowledge of numerous profiles, especially for trace elements, as boron in this case, which are used as useful probes for modern spectroscopic diagnostics. Interpretation of the spectra of white dwarfs, which are very faint, allows understanding the evolution of these very old stars, which are close to death.

The primary results for Stark broadening parameters of BIV lines from 8 spectral series have been calculated using Sahal-Bréchot theory based on the semi-classical perturbation formalism. (Sahal-Bréchot, 1969ab). Within the Sahal-Bréchot theory the full width at half intensity maximum (W) and the shift (d) of an isolated line originating from the transition between the initial level  $i$  and the final level  $f$  is expressed as:

$$W = n_e \int_0^\infty vf(v) dv \left[ \sum_{i' \neq i} \sigma_{ii'}(v) + \sum_{f' \neq f} \sigma_{ff'}(v) + \sigma_{el} \right] \quad (1)$$

$$d = \int_0^\infty vf(v) dv \int_{R_3}^{R_d} 2\pi\rho d\rho \sin 2\varphi_p \quad (2)$$

where  $i'$  and  $f'$  are perturbing levels,  $n_e$  and  $v$  are the electron density and the velocity of perturbers respectively, and  $f(v)$  is the Maxwellian distribution of electron velocities.

The inelastic cross sections  $\sigma_{ii'}(v)$  (respectively  $\sigma_{ff'}(v)$ ) can be expressed by an integration of the transition probability  $P_{ii'}$  over the impact parameter  $\rho$ :

$$\sum_{i' \neq i} \sigma_{ii'}(v) = \frac{1}{2} \pi R_1^2 + \int_{R_1}^{R_d} 2\pi\rho d\rho \sum_{i' \neq i} P_{ii'}(\rho, v) \quad (3)$$

The elastic collision contribution to the width is given by:

$$\sigma_{el} = 2\pi R_2^2 + \int_{R_2}^{R_d} 8\pi\rho d\rho \sin^2 \delta \quad (4)$$

$$\delta = (\varphi_p^2 + \varphi_q^2)^{1/2} \quad (5)$$

The phase shifts  $\varphi_p$  and  $\varphi_q$  are due to the polarization and quadrupole potential respectively. The cut-offs parameters  $R_1$ ,  $R_2$ ,  $R_3$ , the Debye cut-off  $R_d$  and the symmetrization procedure are described in Sahal-Bréchot (1969ab). The collisions of emitters with electrons, protons and ionized helium have been examined, and the contribution of different perturbers in the total Stark broadening parameters have been discussed.

### 3. RESULTS AND DISCUSSION

Stark broadening width and shift for spectral lines of 8 series are presented in Table 1. The temperature dependence of Stark width and shift for the  $1s^2{}^1S - 1s2p {}^1P^\circ$  transition at electron density  $1.10^{18} \text{ cm}^{-3}$  have been presented in Table 1., Fig. 1 and Fig. 2, respectively. The both parameters dramatically change at lower temperature values up to 10 000 K then they vary slowly, the width decreases while the shift increases. The electron contribution in total width decreases from almost 100% to 60%, the proton one increases to 13 %, and the ionized helium one increases too, up to 26 % within the temperature interval of interest. We observe the same tendency for the Stark shift. The contribution of electron perturbers decrease from 97 % to 11 %, the role of collisions with protons increase from 1 % to 27 %, and the ionized helium perturbers broaden the line from 2 % to 72 % in all temperature interval. The values of Stark shift due to collisions with different perturbers are negative in the considered case. The principal quantum dependence of the electron impact width within the series is illustrated in Fig. 3. The examined conditions of interest are 100 000 K and  $1.10^{14} \text{ cm}^{-3}$  electron density. The calculated data are fitted with polynomial function of 4-th order; the fit-curve is added in the figure. The polynomial function permits the interpolation and extrapolation to obtain electron impact width for other lines within the series where there is a lack of the data to perform the calculations. The analytical function is given below:

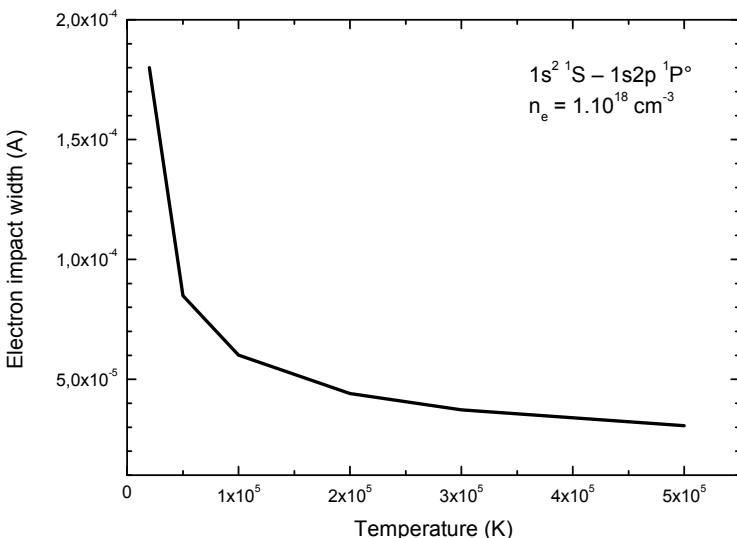


**Figure 1:** Temperature dependence of the electron impact width for  $1s^2{}^1S - 1s2p {}^1P^\circ$  transition at electron density  $1.10^{18} \text{ cm}^{-3}$ .

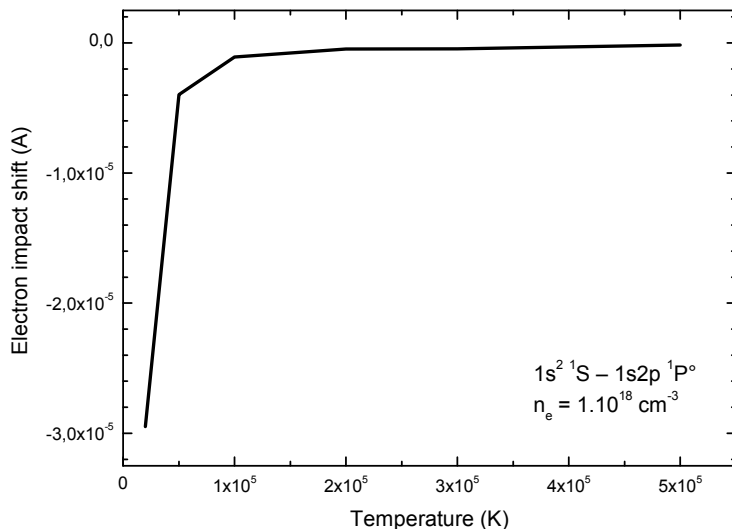


**Figure 2:** Temperature dependence of the electron impact shift for  $1s^2 \ ^1S - 1s2p \ ^1P^\circ$  transition at electron density  $1.10^{18} \text{ cm}^{-3}$ .

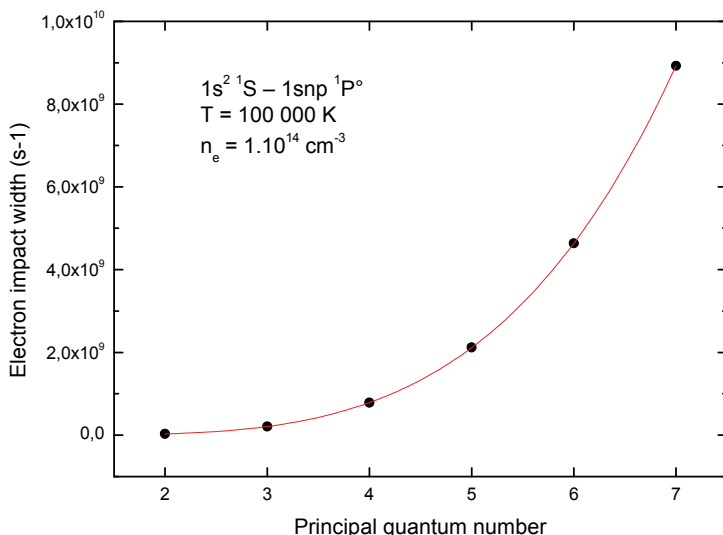


**Figure 3:** Principal quantum dependence of the electron impact width for transitions within  $1s^2 \ ^1S - 1snp \ ^1P^\circ$  series at electron density  $1.10^{14} \text{ cm}^{-3}$  and  $100\ 000 \text{ K}$

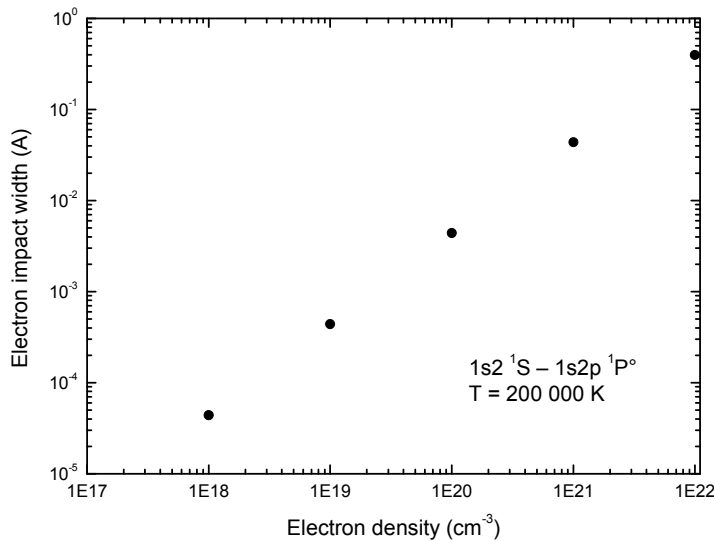


**Figure 4:** Electron density dependence of the electron impact width of  $1s^2 1S - 1s2p 1P^\circ$  transition at 200 000 K.

$$W(n) = a_4 n^4 + a_3 n^3 + a_2 n^2 + a_1 n + a_0 \quad (6)$$

Where  $W(n)$  is the full width at half-maximum in rad.s,  $a_0 = 3.36 \times 10^7$ ,  $a_1 = -2.00 \times 10^7$ ,  $a_2 = 2.96 \times 10^6$ ,  $a_3 = -5.77 \times 10^6$ ,  $a_4 = 4.53 \times 10^6$ . The fitt curve is added in the figure.

The electron density dependence of the electron impact width for  $1s^2 1S - 1s2p 1P^\circ$  transition at 200 000 K have been obtained (see Fig.4). For the electron density values above  $1.10^{21} \text{ cm}^{-3}$  the small deviation from linear function has been observed.

The second studied spectral series in this paper is  $1s2s 1S - 1sn p 1P^\circ$ . We have obtained the similar temperature dependence (see Fig.1) of the electron impact width for the lowest transition within the spectral series,  $1s2s 1S - 1s2p 1P^\circ$ . The variation of Stark width within the studied temperature range has been shown in Fig. 5.

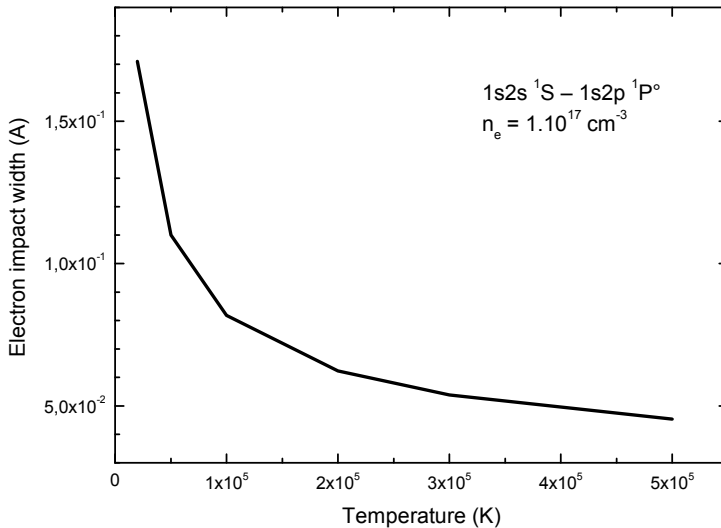


**Figure 5:** Temperature dependence of the electron impact width for  $1s2s ^1S - 1s2p ^1P^\circ$  transition at electron density  $1.10^{17} \text{ cm}^{-3}$ .

The electron contribution in total width decreases from 99 % to 57 %, the proton one increases up to 12 %, and the ionized helium one increases to 30 % in the whole temperature interval. All shift values are negative. The impact electron Stark shift decreases from 61 % to 16 %, the role of collisions with protons increases from 13 % to 22 %, and the ionized helium shift varies from 26 % to 61 %.

#### 4. CONCLUSION

The results for Stark broadening parameters of boron lines could be applicable for the adequate interpretation of the observed spectra to determine reliable chemical boron abundance which is of major importance for the model of Galactic chemical evolution, interstellar and intergalactic space, and stellar interiors and surfaces as white dwarfs.

**Table 1:** Stark broadening parameters for B IV lines for a perturber density  $10^{14}$  cm $^{-3}$  and temperatures from 20 000 to 500 000 K. The width (FWHM)  $W$  and shift  $d$  values from different perturbers are given in (Å). The ratio of the included parameter  $C$  versus the corresponding Stark width estimates the maximal perturber density for which the line may be treated as isolated.  $W_e$  - electron-impact width,  $d_e$  - electron-impact shift,  $W_p$  - proton-impact width,  $d_p$  - proton-impact shift,  $W_{He^+}$  - singly charged helium-impact width,  $d_{He^+}$  - singly charged helium-impact shift.

Transition	T(K)	$W_e$ (Å)	$d_e$ (Å)	$W_p$ (Å)	$d_p$ (Å)	$W_{He^+}$ (Å)	$d_{He^+}$ (Å)
B IV 1s2-2 60.3 Å	20000 50000	0.180E-07 0.860E-08	-0.130E-08 -0.118E-09	0.687E-10 0.211E-09	-0.478E-10 -0.113E-09	0.524E-10 0.204E-09	-0.956E-10 -0.236E-09
C= 0.81E+14	100000 200000 300000 500000	0.601E-08 0.441E-08 0.372E-08 0.306E-08	-0.697E-10 -0.434E-10 -0.447E-10 -0.162E-10	0.365E-09 0.524E-09 0.582E-09 0.658E-09	-0.191E-09 -0.269E-09 -0.317E-09 -0.361E-09	0.470E-09 0.823E-09 0.106E-08 0.131E-08	-0.429E-09 -0.663E-09 -0.805E-09 -0.971E-09
B IV 1s2-3p 52.7 Å	20000 50000	0.584E-07 0.403E-07	-0.434E-08 -0.349E-08	0.282E-08 0.537E-08	-0.387E-08 -0.551E-08	0.496E-08 0.118E-07	-0.956E-08 -0.148E-07
C= 0.39E+13	100000 200000 300000 500000	0.314E-07 0.249E-07 0.218E-07 0.186E-07	-0.316E-08 -0.268E-08 -0.234E-08 -0.196E-08	0.701E-08 0.867E-08 0.976E-08 0.110E-07	-0.665E-08 -0.783E-08 -0.847E-08 -0.947E-08	0.174E-07 0.223E-07 0.250E-07 0.290E-07	-0.179E-07 -0.212E-07 -0.235E-07 -0.260E-07
B IV 1s2-4p 50.4 Å	20000 50000	0.182E-06 0.133E-06	-0.182E-07 -0.166E-07	0.195E-07 0.272E-07	-0.205E-07 -0.261E-07	0.432E-07 0.691E-07	-0.550E-07 -0.704E-07
C= 0.14E+13	100000 200000 300000 500000	0.106E-06 0.854E-07 0.753E-07 0.642E-07	-0.144E-07 -0.115E-07 -0.101E-07 -0.816E-08	0.344E-07 0.408E-07 0.455E-07 0.518E-07	-0.302E-07 -0.354E-07 -0.377E-07 -0.403E-07	0.879E-07 0.108E-06 0.120E-06 0.130E-06	-0.832E-07 -0.974E-07 -0.106E-06 -0.114E-06
B IV 1s2-5p 49.5 Å	20000 50000	0.453E-06 0.340E-06	-0.582E-07 -0.504E-07	0.660E-07 0.898E-07	-0.651E-07 -0.804E-07	0.167E-06 0.232E-06	-0.175E-06 -0.220E-06
C= 0.69E+12	100000 200000 300000 500000	0.275E-06 0.222E-06 0.196E-06 0.166E-06	-0.414E-07 -0.330E-07 -0.279E-07 -0.222E-07	0.101E-06 0.124E-06 0.131E-06 0.146E-06	-0.918E-07 -0.101E-06 -0.117E-06 -0.117E-06	0.277E-06 0.327E-06 0.362E-06 0.407E-06	-0.254E-06 -0.283E-06 -0.305E-06 -0.340E-06
B IV 1s2-6p 48.9 Å	20000 50000	0.915E-06 0.714E-06	-0.143E-06 -0.118E-06	0.170E-06 0.215E-06	-0.159E-06 -0.190E-06	0.434E-06 0.583E-06	-0.430E-06 -0.529E-06
C= 0.40E+12	100000 200000 300000 500000	0.589E-06 0.479E-06 0.422E-06 0.359E-06	-0.948E-07 -0.736E-07 -0.617E-07 -0.481E-07	0.249E-06 0.299E-06 0.304E-06 0.342E-06	-0.216E-06 -0.245E-06 -0.252E-06 -0.278E-06	0.668E-06 0.804E-06 0.870E-06 0.960E-06	-0.592E-06 -0.700E-06 -0.739E-06 -0.846E-06
B IV 1s2-7p 48.6 Å	20000 50000	0.169E-05 0.135E-05	-0.306E-06 -0.238E-06	0.365E-06 0.464E-06	-0.339E-06 -0.398E-06	0.976E-06 0.123E-05	-0.940E-06 -0.113E-05
C= 0.24E+12	100000 200000 300000 500000	0.112E-05 0.917E-06 0.810E-06 0.688E-06	-0.190E-06 -0.143E-06 -0.119E-06 -0.892E-07	0.535E-06 0.578E-06 0.664E-06 0.776E-06	-0.443E-06 -0.521E-06 -0.527E-06 -0.549E-06	0.147E-05 0.175E-05 0.169E-05 0.182E-05	-0.129E-05 -0.143E-05 -0.156E-05 -0.164E-05

**Table 1.** Continued

Transition	T(K)	$W_e(\text{\AA})$	$d_e(\text{\AA})$	$W_p(\text{\AA})$	$d_p(\text{\AA})$	$W_{\text{He}^+}(\text{\AA})$	$d_{\text{He}^+}(\text{\AA})$
B IV 2s-2p	20000	0.168E-03	-0.669E-05	0.702E-06	-0.215E-05	0.642E-06	-0.444E-05
4492.1 A	50000	0.110E-03	-0.577E-05	0.274E-05	-0.417E-05	0.401E-05	-0.959E-05
C= 0.45E+18	100000	0.818E-04	-0.702E-05	0.481E-05	-0.578E-05	0.942E-05	-0.142E-04
	200000	0.623E-04	-0.687E-05	0.712E-05	-0.712E-05	0.168E-04	-0.191E-04
	300000	0.538E-04	-0.673E-05	0.820E-05	-0.787E-05	0.203E-04	-0.213E-04
	500000	0.454E-04	-0.644E-05	0.964E-05	-0.891E-05	0.245E-04	-0.243E-04
B IV 2s-3p	20000	0.336E-05	-0.207E-06	0.150E-06	-0.206E-06	0.266E-06	-0.509E-06
380.9 A	50000	0.233E-05	-0.200E-06	0.286E-06	-0.293E-06	0.627E-06	-0.785E-06
C= 0.20E+15	100000	0.181E-05	-0.189E-06	0.371E-06	-0.353E-06	0.924E-06	-0.947E-06
	200000	0.143E-05	-0.164E-06	0.461E-06	-0.419E-06	0.118E-05	-0.113E-05
	300000	0.126E-05	-0.146E-06	0.518E-06	-0.451E-06	0.134E-05	-0.126E-05
	500000	0.107E-05	-0.125E-06	0.596E-06	-0.506E-06	0.155E-05	-0.139E-05
B IV 2s-4p	20000	0.612E-05	-0.583E-06	0.636E-06	-0.669E-06	0.141E-05	-0.180E-05
288.1 A	50000	0.445E-05	-0.552E-06	0.888E-06	-0.852E-06	0.226E-05	-0.230E-05
C= 0.47E+14	100000	0.355E-05	-0.484E-06	0.112E-05	-0.986E-06	0.287E-05	-0.272E-05
	200000	0.286E-05	-0.390E-06	0.133E-05	-0.116E-05	0.353E-05	-0.318E-05
	300000	0.252E-05	-0.344E-06	0.149E-05	-0.123E-05	0.393E-05	-0.346E-05
	500000	0.215E-05	-0.279E-06	0.170E-05	-0.132E-05	0.426E-05	-0.372E-05
B IV 2s-5p	20000	0.125E-04	-0.158E-05	0.181E-05	-0.178E-05	0.459E-05	-0.479E-05
258.9 A	50000	0.942E-05	-0.139E-05	0.246E-05	-0.220E-05	0.637E-05	-0.604E-05
C= 0.19E+14	100000	0.762E-05	-0.115E-05	0.278E-05	-0.252E-05	0.759E-05	-0.696E-05
	200000	0.615E-05	-0.915E-06	0.339E-05	-0.278E-05	0.895E-05	-0.776E-05
	300000	0.541E-05	-0.775E-06	0.358E-05	-0.322E-05	0.993E-05	-0.835E-05
	500000	0.461E-05	-0.620E-06	0.400E-05	-0.322E-05	0.111E-04	-0.931E-05
B IV 2s-6p	20000	0.231E-04	-0.359E-05	0.428E-05	-0.399E-05	0.109E-04	-0.108E-04
245.3 A	50000	0.180E-04	-0.297E-05	0.540E-05	-0.476E-05	0.147E-04	-0.133E-04
C= 0.99E+13	100000	0.149E-04	-0.239E-05	0.625E-05	-0.542E-05	0.168E-04	-0.149E-04
	200000	0.121E-04	-0.186E-05	0.750E-05	-0.616E-05	0.202E-04	-0.176E-04
	300000	0.107E-04	-0.156E-05	0.764E-05	-0.633E-05	0.219E-04	-0.186E-04
	500000	0.906E-05	-0.122E-05	0.861E-05	-0.698E-05	0.241E-04	-0.213E-04
B IV 2s-7p	20000	0.404E-04	-0.730E-05	0.874E-05	-0.810E-05	0.233E-04	-0.225E-04
237.8 A	50000	0.323E-04	-0.570E-05	0.111E-04	-0.950E-05	0.295E-04	-0.270E-04
C= 0.58E+13	100000	0.269E-04	-0.456E-05	0.128E-04	-0.106E-04	0.351E-04	-0.308E-04
	200000	0.220E-04	-0.342E-05	0.138E-04	-0.125E-04	0.418E-04	-0.341E-04
	300000	0.194E-04	-0.285E-05	0.159E-04	-0.126E-04	0.404E-04	-0.373E-04
	500000	0.165E-04	-0.214E-05	0.185E-04	-0.131E-04	0.435E-04	-0.393E-04
B IV 3s-3p	20000	0.853E-02	-0.604E-03	0.321E-03	-0.455E-03	0.635E-03	-0.113E-02
15513.5 A	50000	0.591E-02	-0.658E-03	0.600E-03	-0.627E-03	0.142E-02	-0.169E-02
C= 0.33E+18	100000	0.462E-02	-0.614E-03	0.776E-03	-0.746E-03	0.197E-02	-0.202E-02
	200000	0.367E-02	-0.553E-03	0.970E-03	-0.877E-03	0.248E-02	-0.241E-02
	300000	0.324E-02	-0.515E-03	0.111E-02	-0.939E-03	0.284E-02	-0.263E-02
	500000	0.277E-02	-0.444E-03	0.120E-02	-0.103E-02	0.327E-02	-0.295E-02

**Table 1.** Continued

Transition	T(K)	$W_e(\text{\AA})$	$d_e(\text{\AA})$	$W_p(\text{\AA})$	$d_p(\text{\AA})$	$W_{\text{He}^+}(\text{\AA})$	$d_{\text{He}^+}(\text{\AA})$
B IV 3s-4p	20000	0.104E-03	-0.983E-05	0.950E-05	-0.100E-04	0.213E-04	-0.270E-04
1098.9 Å	50000	0.749E-04	-0.967E-05	0.133E-04	-0.128E-04	0.338E-04	-0.345E-04
C= 0.68E+15	100000	0.597E-04	-0.854E-05	0.165E-04	-0.147E-04	0.427E-04	-0.409E-04
	200000	0.481E-04	-0.709E-05	0.203E-04	-0.172E-04	0.537E-04	-0.470E-04
	300000	0.424E-04	-0.637E-05	0.223E-04	-0.180E-04	0.597E-04	-0.511E-04
	500000	0.363E-04	-0.525E-05	0.250E-04	-0.194E-04	0.644E-04	-0.560E-04
B IV 3s-5p	20000	0.117E-03	-0.146E-04	0.160E-04	-0.158E-04	0.406E-04	-0.423E-04
767.8 Å	50000	0.877E-04	-0.130E-04	0.218E-04	-0.195E-04	0.560E-04	-0.534E-04
C= 0.17E+15	100000	0.709E-04	-0.108E-04	0.247E-04	-0.224E-04	0.671E-04	-0.617E-04
	200000	0.572E-04	-0.874E-05	0.300E-04	-0.247E-04	0.786E-04	-0.690E-04
	300000	0.504E-04	-0.749E-05	0.321E-04	-0.283E-04	0.879E-04	-0.732E-04
	500000	0.429E-04	-0.603E-05	0.354E-04	-0.285E-04	0.991E-04	-0.825E-04
B IV 3s-6p	20000	0.172E-03	-0.264E-04	0.310E-04	-0.289E-04	0.789E-04	-0.784E-04
659.7 Å	50000	0.134E-03	-0.221E-04	0.391E-04	-0.345E-04	0.106E-03	-0.962E-04
C= 0.72E+14	100000	0.110E-03	-0.178E-04	0.453E-04	-0.393E-04	0.121E-03	-0.108E-03
	200000	0.897E-04	-0.140E-04	0.542E-04	-0.447E-04	0.146E-03	-0.127E-03
	300000	0.791E-04	-0.118E-04	0.550E-04	-0.458E-04	0.158E-03	-0.135E-03
	500000	0.673E-04	-0.923E-05	0.620E-04	-0.503E-04	0.176E-03	-0.154E-03
B IV 3s-7p	20000	0.268E-03	-0.481E-04	0.571E-04	-0.530E-04	0.153E-03	-0.147E-03
608.0 Å	50000	0.214E-03	-0.378E-04	0.725E-04	-0.622E-04	0.193E-03	-0.177E-03
C= 0.38E+14	100000	0.178E-03	-0.303E-04	0.836E-04	-0.693E-04	0.230E-03	-0.201E-03
	200000	0.146E-03	-0.228E-04	0.904E-04	-0.814E-04	0.274E-03	-0.223E-03
	300000	0.129E-03	-0.191E-04	0.104E-03	-0.824E-04	0.265E-03	-0.244E-03
	500000	0.109E-03	-0.144E-04	0.121E-03	-0.858E-04	0.284E-03	-0.257E-03
B IV 4s-4p	20000	0.165	-0.186E-01	0.130E-01	-0.138E-01	0.308E-01	-0.372E-01
37147.1 Å	50000	0.121	-0.178E-01	0.180E-01	-0.175E-01	0.467E-01	-0.472E-01
C= 0.77E+18	100000	0.969E-01	-0.160E-01	0.228E-01	-0.201E-01	0.594E-01	-0.560E-01
	200000	0.784E-01	-0.138E-01	0.263E-01	-0.228E-01	0.710E-01	-0.650E-01
	300000	0.693E-01	-0.122E-01	0.289E-01	-0.249E-01	0.768E-01	-0.682E-01
	500000	0.591E-01	-0.101E-01	0.299E-01	-0.268E-01	0.892E-01	-0.751E-01
B IV 4s-5p	20000	0.132E-02	-0.172E-03	0.161E-03	-0.158E-03	0.405E-03	-0.423E-03
2385.2 Å	50000	0.990E-03	-0.154E-03	0.216E-03	-0.193E-03	0.556E-03	-0.532E-03
C= 0.16E+16	100000	0.801E-03	-0.130E-03	0.260E-03	-0.226E-03	0.691E-03	-0.621E-03
	200000	0.649E-03	-0.108E-03	0.284E-03	-0.243E-03	0.796E-03	-0.693E-03
	300000	0.572E-03	-0.925E-04	0.331E-03	-0.283E-03	0.824E-03	-0.730E-03
	500000	0.487E-03	-0.750E-04	0.339E-03	-0.286E-03	0.102E-02	-0.831E-03
B IV 4s-6p	20000	0.107E-02	-0.166E-03	0.178E-03	-0.167E-03	0.458E-03	-0.455E-03
1580.5 Å	50000	0.830E-03	-0.139E-03	0.227E-03	-0.200E-03	0.614E-03	-0.557E-03
C= 0.41E+15	100000	0.684E-03	-0.114E-03	0.261E-03	-0.229E-03	0.702E-03	-0.633E-03
	200000	0.557E-03	-0.904E-04	0.317E-03	-0.263E-03	0.851E-03	-0.734E-03
	300000	0.492E-03	-0.765E-04	0.312E-03	-0.269E-03	0.942E-03	-0.783E-03
	500000	0.418E-03	-0.603E-04	0.357E-03	-0.292E-03	0.102E-02	-0.888E-03

## ON THE STARK BROADENING OF B IV SPECTRAL LINES

**Table 1.** Continued

Transition	T(K)	$W_e(\text{\AA})$	$d_e(\text{\AA})$	$W_p(\text{\AA})$	$d_p(\text{\AA})$	$W_{\text{He}^+}(\text{\AA})$	$d_{\text{He}^+}(\text{\AA})$
B IV 4s-7p	20000	0.130E-02	-0.235E-03	0.266E-03	-0.248E-03	0.714E-03	-0.688E-03
1313.1 A	50000	0.104E-02	-0.185E-03	0.339E-03	-0.290E-03	0.906E-03	-0.825E-03
C= 0.18E+15	100000	0.866E-03	-0.149E-03	0.390E-03	-0.324E-03	0.108E-02	-0.941E-03
	200000	0.708E-03	-0.113E-03	0.423E-03	-0.382E-03	0.128E-02	-0.104E-02
	300000	0.625E-03	-0.951E-04	0.480E-03	-0.388E-03	0.123E-02	-0.114E-02
	500000	0.532E-03	-0.721E-04	0.565E-03	-0.405E-03	0.132E-02	-0.121E-02
B IV 5s-5p	20000	1.58	-0.251	0.175	-0.172	0.445	-0.462
72971.4 A	50000	1.22	-0.216	0.233	-0.211	0.605	-0.580
C= 0.15E+19	100000	0.998	-0.187	0.273	-0.236	0.711	-0.660
	200000	0.815	-0.151	0.323	-0.279	0.862	-0.772
	300000	0.720	-0.129	0.356	-0.293	0.953	-0.832
	500000	0.613	-0.107	0.379	-0.334	1.05	-0.875
B IV 5s-6p	20000	0.951E-02	-0.163E-02	0.143E-02	-0.137E-02	0.371E-02	-0.368E-02
4401.9 A	50000	0.748E-02	-0.135E-02	0.181E-02	-0.164E-02	0.489E-02	-0.451E-02
C= 0.32E+16	100000	0.620E-02	-0.112E-02	0.211E-02	-0.186E-02	0.562E-02	-0.513E-02
	200000	0.507E-02	-0.884E-03	0.254E-02	-0.208E-02	0.696E-02	-0.592E-02
	300000	0.448E-02	-0.750E-03	0.251E-02	-0.226E-02	0.754E-02	-0.627E-02
	500000	0.382E-02	-0.600E-03	0.277E-02	-0.242E-02	0.830E-02	-0.700E-02
B IV 5s-7p	20000	0.645E-02	-0.126E-02	0.124E-02	-0.116E-02	0.334E-02	-0.319E-02
2809.1 A	50000	0.518E-02	-0.956E-03	0.155E-02	-0.136E-02	0.425E-02	-0.384E-02
C= 0.80E+15	100000	0.433E-02	-0.779E-03	0.181E-02	-0.151E-02	0.503E-02	-0.432E-02
	200000	0.355E-02	-0.594E-03	0.193E-02	-0.178E-02	0.589E-02	-0.475E-02
	300000	0.314E-02	-0.498E-03	0.220E-02	-0.182E-02	0.567E-02	-0.536E-02
	500000	0.267E-02	-0.384E-03	0.259E-02	-0.186E-02	0.589E-02	-0.562E-02
B IV 6s-6p	20000	9.71	-2.14	1.35	-1.28	3.51	-3.47
126390. A	50000	7.79	-1.63	1.72	-1.54	4.67	-4.21
C= 0.26E+19	100000	6.54	-1.34	2.06	-1.76	5.68	-4.91
	200000	5.39	-1.02	2.31	-1.95	6.50	-5.36
	300000	4.77	-0.869	2.55	-2.22	6.89	-5.79
	500000	4.06	-0.702	2.59	-2.49	7.71	-6.54
B IV 6s-7p	20000	0.499E-01	-0.111E-01	0.911E-02	-0.823E-02	0.236E-01	-0.225E-01
7314.1 A	50000	0.405E-01	-0.830E-02	0.112E-01	-0.965E-02	0.298E-01	-0.269E-01
C= 0.55E+16	100000	0.341E-01	-0.669E-02	0.123E-01	-0.106E-01	0.347E-01	-0.307E-01
	200000	0.281E-01	-0.500E-02	0.143E-01	-0.132E-01	0.402E-01	-0.341E-01
	300000	0.248E-01	-0.422E-02	0.157E-01	-0.128E-01	0.423E-01	-0.390E-01
	500000	0.211E-01	-0.330E-02	0.181E-01	-0.135E-01	0.405E-01	-0.428E-01
B IV 7s-7p	20000	45.7	-11.6	7.56	-6.94	20.0	-19.0
201126. A	50000	37.6	-8.59	9.29	-8.41	25.0	-22.8
C= 0.41E+19	100000	32.0	-6.80	9.92	-9.69	30.1	-25.6
	200000	26.5	-5.09	12.7	-10.9	34.0	-29.0
	300000	23.5	-4.30	12.6	-11.1	37.5	-32.8
	500000	20.0	-3.35	13.4	-11.7	41.3	-36.9

**Table 1.** Continued

Transition	T(K)	$W_e(\text{\AA})$	$d_e(\text{\AA})$	$W_p(\text{\AA})$	$d_p(\text{\AA})$	$W_{\text{He}^+}(\text{\AA})$	$d_{\text{He}^+}(\text{\AA})$
B IV 2p-3s	20000	0.366E-05	0.219E-06	0.703E-07	0.139E-06	0.343E-06	0.533E-06
427.7 Å	50000	0.233E-05	0.272E-06	0.167E-06	0.211E-06	0.343E-06	0.533E-06
C= 0.12E+16	100000	0.179E-05	0.256E-06	0.239E-06	0.254E-06	0.602E-06	0.676E-06
	200000	0.141E-05	0.239E-06	0.309E-06	0.303E-06	0.795E-06	0.813E-06
	300000	0.124E-05	0.233E-06	0.345E-06	0.327E-06	0.923E-06	0.905E-06
	500000	0.105E-05	0.201E-06	0.398E-06	0.360E-06	0.108E-05	0.101E-05
B IV 2p-4s	20000	0.521E-05	0.680E-06	0.275E-06	0.370E-06	0.565E-06	0.918E-06
310.5 Å	50000	0.374E-05	0.611E-06	0.457E-06	0.475E-06	0.114E-05	0.128E-05
C= 0.26E+15	100000	0.297E-05	0.573E-06	0.583E-06	0.564E-06	0.152E-05	0.153E-05
	200000	0.239E-05	0.523E-06	0.700E-06	0.652E-06	0.188E-05	0.180E-05
	300000	0.211E-05	0.465E-06	0.761E-06	0.712E-06	0.210E-05	0.196E-05
	500000	0.180E-05	0.390E-06	0.870E-06	0.765E-06	0.237E-05	0.211E-05
B IV 2p-5s	20000	0.912E-05	0.176E-05	0.835E-06	0.905E-06	0.206E-05	0.243E-05
275.7 Å	50000	0.717E-05	0.152E-05	0.116E-05	0.114E-05	0.301E-05	0.308E-05
C= 0.10E+15	100000	0.594E-05	0.136E-05	0.143E-05	0.130E-05	0.390E-05	0.364E-05
	200000	0.488E-05	0.113E-05	0.174E-05	0.151E-05	0.454E-05	0.410E-05
	300000	0.432E-05	0.979E-06	0.188E-05	0.162E-05	0.519E-05	0.451E-05
	500000	0.367E-05	0.827E-06	0.214E-05	0.178E-05	0.533E-05	0.495E-05
B IV 2p-6s	20000	0.164E-04	0.409E-05	0.194E-05	0.199E-05	0.502E-05	0.534E-05
260.0 Å	50000	0.134E-04	0.335E-05	0.257E-05	0.243E-05	0.687E-05	0.678E-05
C= 0.53E+14	100000	0.114E-04	0.287E-05	0.320E-05	0.276E-05	0.844E-05	0.764E-05
	200000	0.948E-05	0.224E-05	0.346E-05	0.319E-05	0.957E-05	0.867E-05
	300000	0.839E-05	0.194E-05	0.409E-05	0.342E-05	0.103E-04	0.949E-05
	500000	0.713E-05	0.161E-05	0.397E-05	0.375E-05	0.122E-04	0.103E-04
B IV 2p-7s	20000	0.281E-04	0.823E-05	0.400E-05	0.399E-05	0.105E-04	0.108E-04
251.4 Å	50000	0.237E-04	0.664E-05	0.540E-05	0.473E-05	0.143E-04	0.134E-04
C= 0.31E+14	100000	0.205E-04	0.531E-05	0.615E-05	0.535E-05	0.168E-04	0.148E-04
	200000	0.171E-04	0.408E-05	0.725E-05	0.612E-05	0.188E-04	0.174E-04
	300000	0.152E-04	0.356E-05	0.762E-05	0.627E-05	0.216E-04	0.183E-04
	500000	0.129E-04	0.285E-05	0.814E-05	0.693E-05	0.209E-04	0.208E-04
B IV 3p-4s	20000	0.117E-03	0.130E-04	0.645E-05	0.776E-05	0.134E-04	0.198E-04
1221.5 Å	50000	0.846E-04	0.126E-04	0.961E-05	0.982E-05	0.248E-04	0.265E-04
C= 0.21E+16	100000	0.675E-04	0.117E-04	0.122E-04	0.116E-04	0.320E-04	0.317E-04
	200000	0.545E-04	0.104E-04	0.150E-04	0.134E-04	0.388E-04	0.366E-04
	300000	0.482E-04	0.916E-05	0.156E-04	0.144E-04	0.448E-04	0.402E-04
	500000	0.411E-04	0.769E-05	0.186E-04	0.155E-04	0.495E-04	0.428E-04
B IV 3p-5s	20000	0.965E-04	0.176E-04	0.793E-05	0.850E-05	0.197E-04	0.228E-04
816.9 Å	50000	0.747E-04	0.150E-04	0.109E-04	0.108E-04	0.285E-04	0.291E-04
C= 0.91E+15	100000	0.616E-04	0.133E-04	0.133E-04	0.123E-04	0.355E-04	0.338E-04
	200000	0.506E-04	0.109E-04	0.161E-04	0.137E-04	0.424E-04	0.390E-04
	300000	0.448E-04	0.947E-05	0.175E-04	0.149E-04	0.474E-04	0.410E-04
	500000	0.381E-04	0.800E-05	0.198E-04	0.165E-04	0.508E-04	0.471E-04

**Table 1.** Continued

Transition	T(K)	$W_e(\text{\AA})$	$d_e(\text{\AA})$	$W_p(\text{\AA})$	$d_p(\text{\AA})$	$W_{\text{He}^+}(\text{\AA})$	$d_{\text{He}^+}(\text{\AA})$
B IV 3p-6s 692.8 Å $C = 0.38E+15$	20000	0.127E-03	0.312E-04	0.141E-04	0.144E-04	0.363E-04	0.386E-04
	50000	0.103E-03	0.248E-04	0.186E-04	0.177E-04	0.504E-04	0.490E-04
	100000	0.877E-04	0.215E-04	0.228E-04	0.200E-04	0.607E-04	0.556E-04
	200000	0.728E-04	0.168E-04	0.251E-04	0.231E-04	0.690E-04	0.631E-04
	300000	0.645E-04	0.143E-04	0.292E-04	0.245E-04	0.744E-04	0.692E-04
B IV 3p-7s 634.8 Å $C = 0.20E+15$	500000	0.548E-04	0.120E-04	0.287E-04	0.270E-04	0.896E-04	0.734E-04
	20000	0.188E-03	0.546E-04	0.258E-04	0.257E-04	0.677E-04	0.692E-04
	50000	0.158E-03	0.437E-04	0.345E-04	0.302E-04	0.922E-04	0.853E-04
	100000	0.136E-03	0.348E-04	0.393E-04	0.342E-04	0.107E-03	0.949E-04
	200000	0.114E-03	0.268E-04	0.465E-04	0.392E-04	0.120E-03	0.112E-03
B IV 4p-5s 2641.1 Å $C = 0.39E+16$	300000	0.101E-03	0.233E-04	0.482E-04	0.400E-04	0.138E-03	0.117E-03
	500000	0.858E-04	0.186E-04	0.519E-04	0.446E-04	0.137E-03	0.135E-03
	20000	0.129E-02	0.209E-03	0.110E-03	0.114E-03	0.275E-03	0.305E-03
	50000	0.992E-03	0.183E-03	0.151E-03	0.144E-03	0.390E-03	0.389E-03
	100000	0.816E-03	0.165E-03	0.177E-03	0.167E-03	0.495E-03	0.450E-03
B IV 4p-6s 1672.5 Å $C = 0.16E+16$	200000	0.669E-03	0.136E-03	0.217E-03	0.188E-03	0.581E-03	0.529E-03
	300000	0.592E-03	0.118E-03	0.239E-03	0.204E-03	0.644E-03	0.564E-03
	500000	0.505E-03	0.986E-04	0.262E-03	0.215E-03	0.729E-03	0.600E-03
	20000	0.852E-03	0.201E-03	0.910E-04	0.911E-04	0.233E-03	0.246E-03
	50000	0.685E-03	0.159E-03	0.122E-03	0.112E-03	0.319E-03	0.309E-03
B IV 4p-7s 1370.5 Å $C = 0.93E+15$	100000	0.579E-03	0.137E-03	0.142E-03	0.126E-03	0.371E-03	0.354E-03
	200000	0.480E-03	0.106E-03	0.167E-03	0.147E-03	0.461E-03	0.409E-03
	300000	0.426E-03	0.913E-04	0.185E-03	0.155E-03	0.494E-03	0.441E-03
	500000	0.362E-03	0.759E-04	0.199E-03	0.178E-03	0.536E-03	0.464E-03
	20000	0.947E-03	0.270E-03	0.127E-03	0.122E-03	0.330E-03	0.331E-03
B IV 4p-7s 1370.5 Å $C = 0.93E+15$	50000	0.789E-03	0.214E-03	0.161E-03	0.146E-03	0.440E-03	0.407E-03
	100000	0.680E-03	0.170E-03	0.186E-03	0.166E-03	0.513E-03	0.456E-03
	200000	0.568E-03	0.131E-03	0.220E-03	0.189E-03	0.601E-03	0.538E-03
	300000	0.504E-03	0.113E-03	0.225E-03	0.195E-03	0.659E-03	0.566E-03
	500000	0.428E-03	0.908E-04	0.246E-03	0.212E-03	0.685E-03	0.650E-03

### Acknowledgments

This paper is a part of the project 176002 "Influence of collisional processes on astrophysical plasma spectra" supported by Ministry of Education and Science of Republic Serbia. The partial financial support from Technical University – Sofia is also acknowledged.

## References

- Cunha, K., Smith, V. V.: 1999, *ApJ*, **512**, 1006.  
Duncan, D. K., Lambert, D. L., Lemke, M.: 1992, *ApJ*, **401**, 584.  
Duncan, D. K., Primas, F., Rebull, L. M., Bøsegaard, A. M., Deliyannis, C. P., Hobbs, L. M., King, J. R.,  
Ritchey, A. M., Federman, S. R., Sheffer, Y., Lambert, D. L.: 2011, *ApJ*, **728**, 70.  
Ryan, S. G.: 1997, *ApJ*, **488**, 338.  
Sahal-Bréchot, S.: 1969a, *Astron. Astrophys.*, **1**, 91.  
Sahal-Bréchot, S.: 1969b, *Astron. Astrophys.*, **2**, 322.  
Sahal-Bréchot, S.: 2010, *J. of Phys.: Conf. Ser.*, **257**, 012028.  
Shima, M.: 1963, *Geochim. Cosmochim. Acta*, **27**, 991.  
Venn, K. A., Brooks, A. M., Lambert, D. L., Lemke, M., Langer, N., Lennon, D. J., Keenan, F. P.: 2002, *ApJ*, **565**, 571.